# A SYSTEMATIC EVALUATION OF DOMAIN ADAPTATION ALGORITHMS ON TIME SERIES DATA

**Anonymous authors**
Paper under double-blind review

## ABSTRACT

Unsupervised domain adaptation methods aim to generalize well on unlabeled test data that may have a different (shifted) distribution from the training data. Such methods are typically developed on image data, and their application to time series data is less explored. Existing works on time series domain adaptation suffer from inconsistencies in evaluation schemes, datasets, and base neural network architectures. Moreover, labeled target data are usually employed for model selection, which violates the fundamental assumption of unsupervised domain adaptation. To address these issues, we propose ADATIME, a standard framework to systematically and fairly evaluate different domain adaptation methods on time series data. Specifically, we standardize the base neural network architectures and benchmarking datasets, while also exploring more realistic model selection approaches that can work with no labeled data or few labeled samples. Our evaluation includes adaptations of state-of-the-art visual domain adaptation methods to time series data in addition to recent methods specifically developed for time series data. We conduct extensive experiments to evaluate 10 state-of-the-art methods on 3 representative datasets spanning 15 cross-domain scenarios. Our results suggest that with careful selection of hyper-parameters, visual domain adaptation methods are competitive with methods proposed for time series domain adaptation. In addition, we find that model selection plays a key role and different selection strategies can significantly affect performance. Our work unveils practical insights for applying domain adaptation methods on time series data and builds a solid foundation for future works in the field.

## 1 INTRODUCTION

Deep learning has achieved a great success in time series classification tasks, assuming access to a vast amount of labeled data for training (Fawaz et al., 2019). However, annotating time series data can be challenging and burdensome due to its complex underlying patterns and complicated domain knowledge (Chang et al., 2020). One way to reduce labeling burden is to leverage annotated data (e.g., synthetic or public data) from a relevant domain (i.e., source domain) to train the model, while testing it on the domain of interest (i.e., target domain). Nevertheless, deep learning tends to perform poorly when tested on unseen data that have different distribution from the training data, which is well-known as the domain shift problem. Considering time series applications, source and target domains usually represent data from different subjects (persons) as in human activity recognition (HAR) (Wilson et al., 2020; Chang et al., 2020) or sleep stage classification (SSC) tasks (Phan et al., 2020). A considerable amount of literature has been developed on Unsupervised Domain Adaptation (UDA), mitigating the domain shift problem for visual applications (Long et al., 2015; Ganin et al., 2016; Long et al., 2018; Chen et al., 2020; Rahman et al., 2020).

Recently, more attention has been paid to time series UDA (TS-UDA) (Wilson et al., 2020; Chang et al., 2020; Ragab et al., 2020; Liu & Xue, 2021). However, the literature of TS-UDA methods suffers from the following limitations. First, most of existing algorithms are mainly *application specific*, and few works have been proposed for TS-UDA in general. As a result, there is a shortage of baseline methods when applying domain adaptation on time series data. Second, prior approaches lack consistent evaluation schemes including benchmark datasets, preprocessing, and backbone networks. For instance, some methods that leverage recurrent neural network as backbone network (Purushotham et al., 2017) are compared against methods with convolutional based backbone net-

works (Wilson et al., 2020). In addition, even with a similar architecture, training procedures can also vary among different algorithms including number of epochs, weight decay, and learning rate schedulers (Tonutti et al., 2019; Purushotham et al., 2017). Therefore, the comparison becomes unfair, and the contribution of the proposed methods might not be evaluated correctly. Finally, while model selection plays a key role in model performance, existing TS-UDA methods mainly rely on labeled data from target domain to select the best hyper-parameters of their models (Wilson et al., 2020; Liu & Xue, 2021). This violates the basic assumption of UDA, i.e., we do not have labelled data in target domain. All the aforementioned challenges can highly affect the performance and can be mistakenly attributed to the proposed domain adaptation methods.

In this work, we propose ADATIME, which provides a systematic evaluation framework to tackle the aforementioned obstacles and remove all extraneous factors to ensure a fair evaluation of different UDA algorithms on time series data. Specifically, we first standardize the preparation and processing of three benchmarking datasets from two classic real-world applications, including healthcare and human activity recognition. Second, to address the lack of TS-UDA baselines, we re-implement various state-of-the-art visual UDA methods that can be adapted to time series data while comparing to the existing TS-UDA methods. Finally, we explore more realistic model selection strategies for TS-UDA problem. Particularly, we investigate the model performance when selecting models based on source dataset (i.e., source risk (Ganin et al., 2016)), unlabeled target data (i.e., deep embedded evaluation (DEV) (You et al., 2019)), or only few-shot labeled samples from target data.

Given our standard framework, we aim to systematically study the the following questions: (1) With standard backbone network and evaluation schemes, how will the visual UDA methods perform on time series data; (2) Can we use realistic model selection methods —relying on only few or no target labels— and still achieve acceptable adaptation performance on time series data; (3) How can the backbone network contribute to the performance. In this paper, we conduct comprehensive experiments to answer the aforementioned three questions. Some of our findings are summarized as follows:

- Visual domain adaptation methods can achieve comparable or even better performance than the methods proposed for time series data. Furthermore, with sufficient amount of training and testing data, domain adaptation methods tend to achieve similar performance.
- Unlike image data, selecting models based on source risk can achieve reasonable performance and outperforms the DEV risk for time series data. Additionally, we find that our proposed few-shot target risk can achieve comparable performance to target risk, with affordable few labels samples.
- Changing the base architecture can be pivotal to the performance. Moreover, complex architectures with time series data can have lower generalization performance on cross-domain experiments.

## 2 DOMAIN ADAPTATION PROBLEM

We start by defining the unsupervised domain adaptation problem. We assume the access to a labeled source domain $\mathcal{X}_s = \{(\mathbf{x}_i^s, y_i^s)\}_{i=1}^{N_s}$ that represents univariate or multivariate time series data, and unlabeled target domain $X_t = \{(\mathbf{x}_i^t)\}_{i=1}^{N_t}$ where $N_s$ and $N_t$ denote the number of samples for $X_s$ and $X_t$ respectively. The source and target domains are sampled from different marginal distributions $P_s(x) \neq P_t(x)$ while the conditional distribution $P_s(y|x) = P_t(y|x)$ remains stable. The main goal of UDA is to address the distribution shift between $P_s(x)$ and $P_t(x)$, assuming they shared the same label space. Particularly, UDA algorithms leverage labeled source domain to improve the performance on unlabeled target domains.

The mainstream of UDA algorithms are addressing the domain shift problem via finding domain invariant feature representation. Formally, given a backbone model $f_\theta : X \to Z$, which transforms the input space to the feature space. The UDA algorithm is mainly optimize the backbone network to find new invariant representation for the target features such that $P_s(f_\theta(x)) = P_t(f_\theta(x))$. As a results, a model trained on the source domain can generalize well to the adapted target domain.

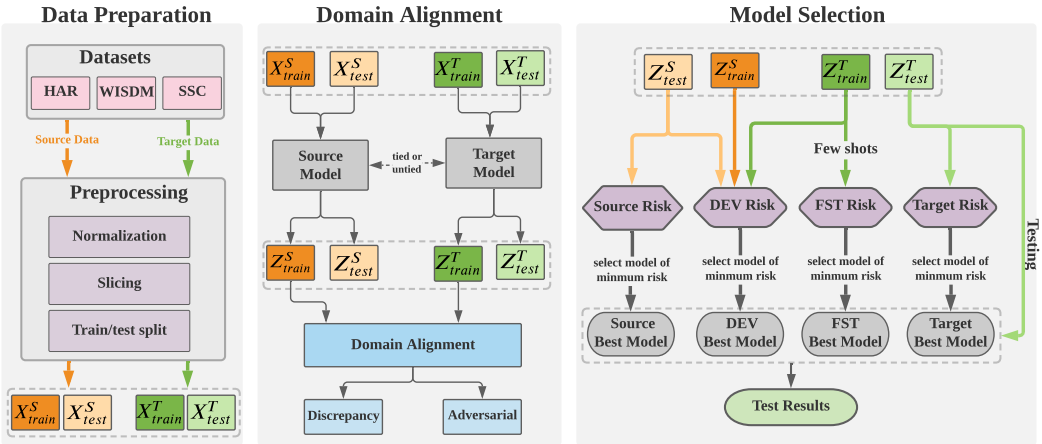


Figure 1: The details of ADATIME framework for time series domain adaptation. (Best viewed in colors)

## 3 ADATIME: A BENCHMARKING APPROACH FOR TIME SERIES DOMAIN ADAPTATION

In this work, we systematically evaluate domain adaptation algorithms on time series data, ensuring fair and realistic procedures. Figure 1 shows the details of ADATIME, which proceeds as follows. Given a dataset, we first apply our standard time series preparation schemes on the selected source and target domains. Subsequently, the source and target train data are passed through our backbone network to extract features from source and target domains. The selected UDA algorithm is then applied to the extracted features to mitigate the distribution shift between the two domains. We select the hyper-parameters of the model that achieves the minimum risk with one of the selection strategies: source risk, DEV risk, few-shot target risk, and target risk. Last, we test the selected best model on the test set of the target domain. The code of ADATIME will be made publicly available for researchers to enable seamless evaluation of different domain adaptation methods on time series data.

### 3.1 BACKBONE NETWORK

The general domain adaptation network consists of a feature extractor, a classifier, as well as different components to align the domains. We refer to the feature extractor and the classifier as the backbone network. The backbone network can have a pivotal contribution to the UDA model performance, as using different architectures may result in different performance. Hence, changing the backbone network when comparing different UDA methods can result in misleading outcomes, which can hinder the fair evaluation protocol. In most visual applications, ResNet-50 is the dominantly adopted feature extractor, as its complex architecture can extract representative features from images. However, in time series, using such complex architectures can lead to overfitting problems (Fawaz et al., 2019). Therefore, we use a simple CNN architecture in ADATIME (see Figure 6) , and study the effect of different backbone architectures on the performance of TS-UDA methods.

### 3.2 DOMAIN ADAPTATION ALGORITHMS

While numerous UDA approaches have been proposed to address the domain shift problem (Zhao et al., 2020b), a comprehensive review of existing UDA methods is out of our scope. Instead, we only included the most solid and recent baselines for visual UDA that can be adapted to time series. Besides, we include the state-of-the-art methods proposed for time series data. Overall, the selected algorithms in ADATIME can fit into two main categories, namely discrepancy based methods and adversarial based methods. The former aims to minimize a statistical distance between source and target features to mitigate the domain shift problem (Tzeng et al., 2014; Sun & Saenko, 2016; Chen et al., 2020). The latter leverages a domain discriminator network that enforces the feature extractor

to produce domain invariant features (Ganin et al., 2016; Tzeng et al., 2017). Each method in the above categories can also be classified according to the aligned distribution. Specifically, some algorithms only align the marginal distribution of the feature space, while other algorithms jointly align the marginal and conditional distributions.

The selected UDA algorithms are as follows: Deep Domain Confusion (**DDC** Tzeng et al. (2014)); Higher-order Moment Matching (**HoMM** Zhao et al. (2020a)); Correlation Alignment via Deep Neural Networks (**Deep-CORAL** Sun et al. (2017)); Minimum Discrepancy Estimation (**MMDA** Rahman et al. (2020)); Domain-Adversarial Training of Neural Networks (**DANN** Ganin et al. (2016)); Conditional Adversarial Domain Adaptation (**CDAN** Long et al. (2018)); Deep Subdomain Adaptation (**DSAN** Zhu et al. (2021)); (**DIRT-T** Shu et al. (2018)). In addition, we also include two TS-UDA methods, which are **CoDATS** (Wilson et al., 2020) and **AdvSKM** (Liu & Xue, 2021), noting that there are very few TS-UDA methods in the literature. Most of the TS-UDA methods just adopt the approaches developed in visual UDA. Table 1 shows a summary of the selected methods and their corresponding categories.

Table 1: Summary of Domain Adaptation algorithms used for our benchmarking framework

| **Algorithm** | **Application** | **Category** | **Distribution** | **Losses** |
|---|---|---|---|---|
| DDC (Tzeng et al., 2014) | Visual | Discrepancy | Marginal | MMD |
| Deep-Coral (Sun & Saenko, 2016) | Visual | Discrepancy | Marginal | CORAL |
| HoMM (Chen et al., 2020) | Visual | Discrepancy | Marginal | High-order MMD |
| MMDA (Rahman et al., 2020) | Visual | Discrepancy | Joint | MMD,<br>CORAL,<br>Entropy |
| DSAN (Zhu et al., 2021) | Visual | Discrepancy | Joint | Local MMD |
| DANN (Ganin et al., 2016) | Visual | Adversarial | Marginal | Domain Classifier,<br>Gradient Reversal Layer |
| CDAN (Long et al., 2018) | Visual | Adversarial | Joint | Conditional adversarial<br>Domain Classifier |
| DIRT-T (Shu et al., 2018) | Visual | Adversarial | Joint | Virtual adversarial<br>Entropy<br>Domain Classifier |
| CoDATS (Wilson et al., 2020) | Time Series | Adversarial | Marginal | Domain Classifier,<br>Gradient Reversal Layer |
| AdvSKM (Liu & Xue, 2021) | Time Series | Adversarial | Marginal | Spectral Kernel<br>Adversarial MMD |

### 3.3 Model Selection Approaches

Model selection and hyper-parameter tuning for UDA are long standing non-trivial problems due to the lack of target domain labels. However, very few works have been proposed to address these issues. Some of UDA methods use a labeled (validation) set from the target domain to select the best hyper-parameters (Shu et al., 2018; Saito et al., 2017), which can be infeasible in real-world scenarios and violates the fundamental assumption of UDA. Similar to theses methods, TS-UDA methods also use target domain validation set for hyper-parameters tuning. In this section, we explore realistic model selection approaches that could be applied for TS-UDA without the need of any target domain labels, such as: source risk (Ganin et al., 2016) and deep embedded validation (DEV) risk (You et al., 2019). Besides, we propose few-shot target risk, which utilizes a few labeled samples from the target domain that can be obtained with affordable efforts. We compare all the aforementioned risks with the target risk. Detailed explanation of each risk can be found as follows:

**Source Risk (SRC Risk)** In this approach, we choose the model that achieves the minimum risk on test set of the source data. This approach can be easily applicable without additional labeling efforts, since it relies on the existing labeled source data Ganin et al. (2016). However, the performance of

source risk is mainly affected by the sample size of source data and severity of distribution shift between the source and target domains.

**Deep Embedded Validation (DEV Risk)** This approach tries to yield unbiased estimation to the target risk. The key idea is to consider the relationship between the source and target data when calculating the risk. Particularly, DEV risk considers the source features that are highly correlated to the target features via importance weighting schemes. By ranking candidate models based on their computed DEV risks, the model with the smallest DEV risk is chosen as the best candidate model to be used for adaptation.

**Few-Shot Target Risk (FST Risk)** We propose few-shot target risk as a relaxed target risk. While labeling of vast amount of time series data can be laborious, annotating few-shot samples can still be affordable. We use these samples as a validation to select the best hyper-parameters.

**Target Risk (TGT Risk)** This approach involves leaving out a subset of the target domain samples and their labels as a validation set, and uses them to select the best performing hyper-parameters on the target domain. This represents the upper bound that the UDA method can achieve on the target domain. This risk has been used by many UDA methods for model selection (Shu et al., 2018; Saito et al., 2017), which is impractical.

# 4 EXPERIMENTS

## 4.1 BENCHMARKING DATASETS

We evaluate the various UDA algorithms on three benchmark datasets from two real-world applications, namely human activity recognition and sleep stage classification. The benchmark datasets span range of different characteristics including complexity, type of sensors, sample size, class-distribution, and severity of shift, enabling more broad evaluation. The selected datasets are detailed as follows:

**UCIHAR (Anguita et al., 2013)** UCIHAR is one of the most widely used datasets to evaluate performance on time series data. It contains three different sensors namely, accelerometer, gyroscope, and body sensors. These sensors have been used to collect data from 30 different persons. In our experiments, we treat each subject as a separate domain. Due to the large number of cross-domain combinations, we randomly selected five cross domain scenarios, as in (Liu & Xue, 2021; Wilson et al., 2020).

**WISDM (Kwapisz et al., 2011)** WISDM is another popular activity recognition dataset for the evaluation of time series domain adaptation. In this dataset, accelerometer sensors were applied to collect data from 36 subjects. This data can be more challenging because of the class imbalance issue among different subjects. Particularly, some subjects may contain only samples from a subset of the overall classes. Further detailed about ratio of different classes among subjects can be found in the Appendix. Similar to UCIHAR dataset, we consider each subject as a separate domain and we randomly select five cross-domain scenarios.

**SSC (Goldberger et al., 2000)** Sleep stage classification (SSC) problem aims to classify the electroencephalography (EEG) signals into five stages i.e. Wake (W), Non-Rapid Eye Movement stages (N1, N2, N3), and Rapid Eye Movement (REM). We adopted Sleep-EDF dataset (Goldberger et al., 2000), which contains EEG readings from 20 healthy subjects. We selected a single channel (i.e., Fpz-Cz) following previous studies (Eldele et al., 2021a), and 10 different subjects to construct five subject-wise cross-domain scenarios.

Table 2 summarizes the details of each dataset, e.g., the number of selected domains, the number of sensor channels, the number of classes, as well as the average number of samples per domain in both training and test portions.

Table 2: Details of datasets. More details about selected cross-domain scenarios for each dataset cab be found in Tables 4, 5, and 6.

| Dataset | Number of | | | | Avg # samples per domain | |
|---|---|---|---|---|---|---|
| | Domains | Channels | Classes | Timesteps/sample | Training set | Testing set |
| UCIHAR | 10 | 9 | 6 | 128 | 230 | 99 |
| WISDM | 9 | 3 | 6 | 128 | 150 | 80 |
| SSC | 10 | 1 | 5 | 3000 | 1,428 | 613 |

### 4.2 Experimental Setup

**Hyper-parameter Sweep** For each algorithm and dataset, we conducted extensive random hyper-parameter search with 100 trials. The hyper-parameters are picked by uniformly sampling from a range of predefined values. Details about the specified ranges can be found in Table 7 in the appendix). In addition, for each set of hyper-parameters, we calculate the risk values over three different random seeds, removing the bias to a single seed. We pick the model that achieves the minimum risk value for each model selection strategy. For few-shot target risk experiments, we use five samples per class in each dataset to compute the risk.

**Datasets Preprocessing** The preprocessing of time series data includes data slicing, train/test splitting, normalization. To promote fair evaluation, we preserve consistency among all the aforementioned processing steps when comparing between different UDA algorithms. In our experiments, we use a sliding window of 128 for human activity recognition datasets. For SSC dataset, we keep the original sample length of 3000 time steps. Next, we split both source and target domains into train/test splits with a ratio of 0.7/0.3 respectively. Finally, we normalize both training and testing data based on the training statistics (Wilson et al., 2020; Liu & Xue, 2021). It worth noting that WISDM dataset is severely imbalanced among different subjects (see Figure 4(b) in the appendix), with some classes are not available for some subjects. To stabilize the training, we select subjects that contain samples from all the classes when constructing the source and target domains.

**Backbone Network** To ensure a fair evaluation among all the baselines, we use a fixed backbone network among all the compared UDA methods in our implementation. We employ a 3-layer 1D-CNN with adaptive average pooling, to handle signals with different lengths, as a feature extractor. This architecture is commonly used in series applications Wilson et al. (2020); Eldele et al. (2021b). We adopt a single layer fully connected network as the classifier. Yet, to include CoDATS in our experiments, we use a 3-layer fully connected classifier (as proposed in their work) to differentiate it from DANN.

**Training Procedure** All the training procedures have been standardized across all UDA algorithms. For instance, we train our models for 40 epochs, as performance tends to decrease with longer training. We report the model performance after completing the last epoch. Regarding the optimization of the model, we use Adam optimizer with a fixed weight decay of $1e-4$ and $(\beta_1, \beta_2) = (0.5, 0.99)$. The learning rate is set to be a tunable hyper-parameter for each method on each dataset. We excluded any learning rate scheduling schemes from our experiments to ensure that the contribution is mainly attributed to the selected UDA algorithm.

## 5 Results Discussion

We conduct extensive experiments for each UDA method on all the datasets. The average F1-score of the five cross-domain scenarios for each dataset and each UDA algorithm is shown in Table 3. We also show the results of each risk to compare the performance to the target risk. Detailed versions of Table 3 can be found in Tables 4, 5, and 6) in the appendix. We further discuss the results in the following paragraphs.

**Visual UDA methods achieve comparable performance to TS-UDA methods on time series data.** Table 3 shows the performance of adapted visual UDA methods and existing TS-UDA meth-

Table 3: The average results (from 5 cross-domain scenarios) according to the minimum risk value in terms of MF1-score.

| Dataset | Algorithm | SRC Risk | DEV Risk | FST Risk | TGT Risk | Avg/alg |
|---|---|---|---|---|---|---|
| UCIHAR | DDC | 68.83 | 74.14 | 74.25 | 75.67 | 73.22 |
| | Deep-Coral | 71.99 | 71.43 | 77.23 | 77.71 | 74.59 |
| | HoMM | 75.86 | 78.28 | 81.3 | 84.1 | 79.89 |
| | MMDA | 80.12 | 80.12 | 79.54 | 81.4 | 80.30 |
| | DSAN | 83.31 | 81.07 | 87.13 | 90.96 | 85.62 |
| | DANN | 79.82 | 80.89 | 83.1 | 84.97 | 82.20 |
| | CDAN | 86.55 | 64.66 | 86.79 | 86.79 | 81.20 |
| | DIRT-T | **86.72** | **82.54** | **88.47** | **92.2** | **87.48** |
| | CoDATS | 79.05 | 65.12 | 79.1 | 85.47 | 77.19 |
| | AdvSKM | 71.08 | 74.62 | 74.47 | 74.67 | 73.71 |
| | Avg/risk | 78.33 | 75.29 | 81.14 | 83.39 | |
| WISDM | DDC | 51.94 | 52.23 | 49.11 | 58.24 | 52.88 |
| | Deep-Coral | 52.99 | 52.98 | 49.48 | 60.19 | 53.91 |
| | DANN | 56.10 | 53.87 | 49.78 | 63.67 | 55.86 |
| | HoMM | 54.13 | **61.17** | 52.67 | 62.98 | 57.74 |
| | CDAN | 53.69 | 53.47 | 54.68 | 57.69 | 54.88 |
| | MMDA | **58.82** | 53.49 | 51.18 | 63.97 | 56.87 |
| | DSAN | 56.20 | 56.20 | 58.82 | 61.46 | 58.17 |
| | DIRT-T | 56.26 | 54.95 | **67.42** | **67.42** | **61.51** |
| | CoDATS | 55.57 | 56.24 | 50.20 | 63.58 | 56.40 |
| | AdvSKM | 57.43 | 53.23 | 48.31 | 60.55 | 54.88 |
| | Avg/risk | 53.93 | 53.52 | 51.91 | 60.82 | |
| SSC | DDC | 61.11 | 61.39 | **61.41** | 61.48 | **61.44** |
| | Deep-Coral | 61.42 | 61.36 | 61.36 | 61.42 | 61.39 |
| | HoMM | 61.31 | 60.95 | 61.31 | 61.31 | 61.22 |
| | MMDA | **62.13** | 61.49 | 59.77 | 62.23 | 61.41 |
| | DSAN | 61.46 | **61.70** | 60.45 | **62.28** | 61.39 |
| | DANN | 60.61 | 57.96 | 60.61 | 60.61 | 59.95 |
| | CDAN | 57.86 | 60.42 | 57.96 | 60.78 | 59.26 |
| | DIRT-T | 59.38 | 60.58 | 58.90 | 60.95 | 59.95 |
| | CoDATS | 56.76 | 55.79 | 54.64 | 58.45 | 56.41 |
| | AdvSKM | 60.34 | 60.35 | 60.22 | 60.36 | 60.32 |
| | Avg/risk | 59.37 | 59.34 | 59.10 | 60.30 | |

ods. Surprisingly, with standardizing the backbone network, we find that visual UDA methods achieve competitive performance or even outperform TS-UDA methods. This finding is consistent for all the model selection strategies across the three benchmarking datasets. A possible explanation is that all selected UDA algorithms are applied on the vectorized output features of the backbone network, which can be independent from the input data modality. This finding suggests that with a standard backbone network, visual UDA algorithms can be strong baselines for TS-UDA.

**Methods with joint distribution alignment tend to perform consistently better.** As shown in Table 1, Methods that address the joint distributions (i.e., both marginal and conditional distributions concurrently) such as DIRT-T, MMDA, and DSAN, achieve the state-of-the-art performance on the three datasets, outperforming TS-UDA methods. For example, the best performing method, as selected by the target risk, is DIRT-T in both UCIHAR and WISDM datasets, and DSAN in SSC dataset. Similarly, with respect to the different risks, DIRT-T, MMDA, and DSAN are interchangeably achieving performing best across the benchmarking datasets. Hence, considering the conditional distribution when aligning the source and target can be beneficial to the performance.

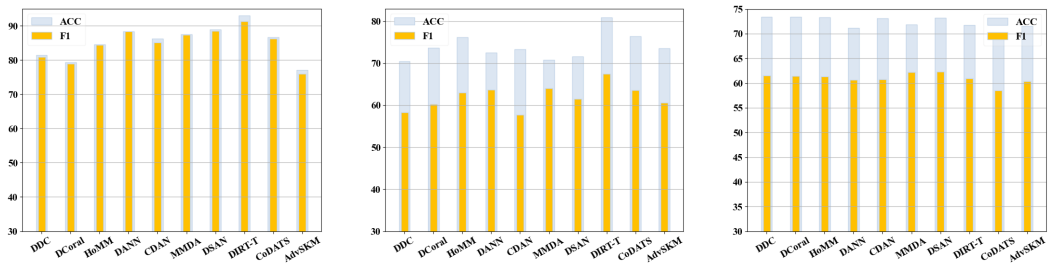


(a) UCIHAR dataset (b) WISDM dataset (c) SSC dataset

Figure 2: Results of best models according to target risk for different methods in terms of accuracy and macro average F1-score.

**Performance Gap diminishes with sufficient amount of data.** In Figure 2, we plot the accuracy and F1-score of the best performing models for each method according to the target risk. We find that for datasets with smaller sample size such as UCIHAR and WISDM datasets, there exists a large performance gap between different methods in terms of both accuracy and F1-score, as shown in Figures 2(a) and 2(b). In contrast, for datasets with larger sample size such as SSC dataset, performance gap is becoming much smaller between different UDA algorithms, as shown in Figure 2(c). Therefore, we conclude that with sufficient amount of data and standard evaluation protocols, different domain adaptation methods tend to achieve similar performance on time series data.

**Model selection has a significant effect on the performance.** Model selection strategies can yield different performance for the same UDA algorithm, as shown in Table 3. This reveals the significant contribution of model selection approach to the overall performance. While target risk achieves superior performance, it is infeasible for practical scenarios with no target labels available. Surprisingly, source risk can achieve a comparable performance to the target risk on UCIHAR and SSC datasets. In addition, with affordable labeling efforts, our proposed few-shot target risk can also achieve a compititive performance to the target risk. However, for severely imbalanced WISDM dataset, different model selection approaches fail to follow the target risk performance.

**Backbone network can be pivotal to the performance.** To investigate the influence of the backbone network on the method's performance, we evaluate all the UDA algorithms under two different backbone networks. Particularly, we employ 1D-CNN (described in Section 4.2) and 1D-ResNet-18 (i.e., a standard ResNet-18 with 1D convolutional kernel) as backbone networks. The two architectures are different in terms of their complexity and number of trainable parameters. Figure 3 shows a comparison of different UDA algorithms under two backbone architectures. Clearly, changing the backbone network can contribute significantly to the performance. In addition, using a simpler 1D-CNN architecture can have higher generalization capability for TS-UDA. This may be explained by the fact that time series data have much lower dimensionality compared to image data, such that complex models tend to suffer from overfitting problem.

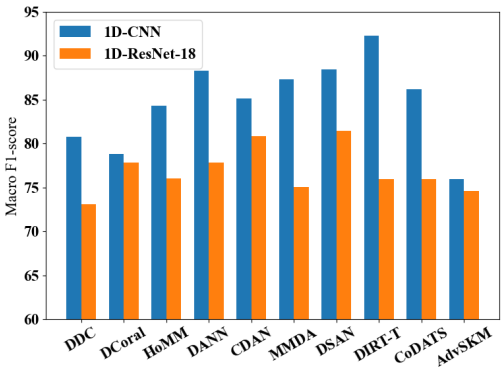


Figure 3: Comparison between 1D-CNN and 1D-ResNet-18 backbones applied on the UCIHAR dataset. Results are in terms of macro F1-score.

**Accuracy metric should not be used to measure performance for imbalanced data.** While it is well known that accuracy is not a representative metric for class-imbalanced datasets, existing TS-UDA methods are still relying on it to measure the performance (Chang et al., 2020; Wilson

et al., 2020; Liu & Xue, 2021). We aim to re-emphasize that considering the imbalanced nature in most time series data, the accuracy metric can give over-optimistic results. For example, in Figure 2(b), although CDAN achieves higher accuracy than some other methods such as DDC, MMDA and DSAN, it performs the worst in terms of F1-score. In contrast, with a balanced dataset (i.e., UCIHAR), as shown in Figure 2(a), accuracy can still be representative and achieve similar performance to F1-Score.

## 6 Conclusions and Recommendations

In this work, we provided AdaTime for a systematic evaluation of the existing domain adaptation methods on time series data. To ensure fair and realistic evaluation, we standardized the benchmarking dataset, evaluation schemes, and backbone networks among different domain adaptation methods. Moreover, we explored more realistic model selection approaches that can work with no labels or only few-shot labeled samples. Based on our systematic study and unveiled findings, we suggest the following recommendations:

- Future research on time series domain adaptation should consider visual UDA methods as strong baselines.
- Considerable amount of target labels should not be used for the UDA model selection. Instead, source risk or few-shot target risk can be better candidates for a more realistic model selection approach.
- The backbone network should be fixed when comparing between different UDA methods. In addition, simpler models should used with time series data to achieve a higher generalization ability.
- Larger datasets should be considered when comparing baselines to obtain reliable results.
- Accuracy metric should no longer be used to evaluate imbalance datasets, as it can yield misleading results.

## References

Davide Anguita, Alessandro Ghio, Luca Oneto, Xavier Parra, and Jorge Luis Reyes-Ortiz. A public domain dataset for human activity recognition using smartphones. In *European Symposium on Artificial Neural Networks*, pp. 437–442, 2013.

Youngjae Chang, Akhil Mathur, Anton Isopoussu, Junehwa Song, and Fahim Kawsar. A systematic study of unsupervised domain adaptation for robust human-activity recognition. *Proceedings of the ACM on Interactive, Mobile, Wearable and Ubiquitous Technologies*, 4(1):1–30, 2020.

Chao Chen, Zhihang Fu, Zhihong Chen, Sheng Jin, Zhaowei Cheng, Xinyu Jin, and Xian-Sheng Hua. Homm: Higher-order moment matching for unsupervised domain adaptation. *AAAI*, 2020.

Emadeldeen Eldele, Zhenghua Chen, Chengyu Liu, Min Wu, Chee-Keong Kwoh, Xiaoli Li, and Cuntai Guan. An attention-based deep learning approach for sleep stage classification with single-channel eeg. *IEEE Transactions on Neural Systems and Rehabilitation Engineering*, 2021a. doi: 10.1109/TNSRE.2021.3076234.

Emadeldeen Eldele, Mohamed Ragab, Zhenghua Chen, Min Wu, Chee Keong Kwoh, Xiaoli Li, and Cuntai Guan. Time-series representation learning via temporal and contextual contrasting. In *Proceedings of the Thirtieth International Joint Conference on Artificial Intelligence, IJCAI-21*, pp. 2352–2359, 2021b.

Hassan Ismail Fawaz, Germain Forestier, Jonathan Weber, Lhassane Idoumghar, and Pierre-Alain Muller. Deep learning for time series classification: a review. *Data Mining and Knowledge Discovery*, 33(4):917–963, 2019.

Yaroslav Ganin, Evgeniya Ustinova, Hana Ajakan, Pascal Germain, Hugo Larochelle, François Laviolette, Mario Marchand, and Victor Lempitsky. Domain-adversarial training of neural networks. *The Journal of Machine Learning Research*, 17(1):2096–2030, 2016.

Yaroslav Ganin, Evgeniya Ustinova, Hana Ajakan, Pascal Germain, Hugo Larochelle, François Laviolette, Mario Marchand, and Victor Lempitsky. Domain-adversarial training of neural networks. *JMLR*, 17(1):1–35, 2016.

Ary L. Goldberger, Luis A. N. Amaral, Leon Glass, Jeffrey M. Hausdorff, Plamen Ch. Ivanov, Roger G. Mark, Joseph E. Mietus, George B. Moody, Chung-Kang Peng, and H. Eugene Stanley. Physiobank, physiotoolkit, and physionet components of a new research resource for complex physiologic signals. *Circulation*, 101(23):215–220, 2000.

Jennifer R. Kwapisz, Gary M. Weiss, and Samuel A. Moore. Activity recognition using cell phone accelerometers. *Sigkdd Explorations*, 12(2):74–82, 2011.

Qiao Liu and Hui Xue. Adversarial spectral kernel matching for unsupervised time series domain adaptation. In *Proceedings of the Thirtieth International Joint Conference on Artificial Intelligence, IJCAI-21*, 2021.

Mingsheng Long, Yue Cao, Jianmin Wang, and Michael Jordan. Learning transferable features with deep adaptation networks. In *International conference on machine learning*, pp. 97–105. PMLR, 2015.

Mingsheng Long, Zhangjie Cao, Jianmin Wang, and Michael I. Jordan. Conditional adversarial domain adaptation. In *NeurIPS*, 2018.

Huy Phan, Kaare Mikkelsen, Oliver Y Chén, Philipp Koch, Alfred Mertins, Preben Kidmose, and Maarten De Vos. Personalized automatic sleep staging with single-night data: a pilot study with kullback-leibler divergence regularization. *Physiological Measurement*, 41(6):64004, 2020.

Philipp Probst, Anne-Laure Boulesteix, and Bernd Bischl. Tunability: importance of hyperparameters of machine learning algorithms. *The Journal of Machine Learning Research*, 20(1): 1934–1965, 2019.

Sanjay Purushotham, Wilka Carvalho, Tanachat Nilanon, and Yan Liu. Variational recurrent adversarial deep domain adaptation. In *ICLR 2017 : International Conference on Learning Representations 2017*, 2017.

Mohamed Ragab, Zhenghua Chen, Min Wu, Haoliang Li, Chee-Keong Kwoh, Ruqiang Yan, and Xiaoli Li. Adversarial multiple-target domain adaptation for fault classification. *IEEE Transactions on Instrumentation and Measurement*, 70:1–11, 2020.

Mohammad Mahfujur Rahman, Clinton Fookes, Mahsa Baktashmotlagh, and Sridha Sridharan. On minimum discrepancy estimation for deep domain adaptation. *Domain Adaptation for Visual Understanding*, 2020.

Kuniaki Saito, Yoshitaka Ushiku, and Tatsuya Harada. Asymmetric tri-training for unsupervised domain adaptation. In *ICML'17 Proceedings of the 34th International Conference on Machine Learning*, pp. 2988–2997, 2017.

Rui Shu, Hung Bui, Hirokazu Narui, and Stefano Ermon. A dirt-t approach to unsupervised domain adaptation. In *International Conference on Learning Representations*, 2018.

Baochen Sun and Kate Saenko. Deep coral: Correlation alignment for deep domain adaptation. In *ECCV*, pp. 443–450. Springer, 2016.

Baochen Sun, Jiashi Feng, and Kate Saenko. Correlation alignment for unsupervised domain adaptation. In *Domain Adaptation in Computer Vision Applications*, pp. 153–171. Springer, 2017.

Michele Tonutti, Emanuele Ruffaldi, Alessandro Cattaneo, and Carlo Alberto Avizzano. Robust and subject-independent driving manoeuvre anticipation through domain-adversarial recurrent neural networks. *Robotics and Autonomous Systems*, 115:162–173, 2019.

Eric Tzeng, Judy Hoffman, Ning Zhang, Kate Saenko, and Trevor Darrell. Deep domain confusion: Maximizing for domain invariance. *arXiv preprint arXiv:1412.3474*, 2014.

Eric Tzeng, Judy Hoffman, Kate Saenko, and Trevor Darrell. Adversarial discriminative domain adaptation. In *Proceedings of the IEEE conference on computer vision and pattern recognition*, pp. 7167–7176, 2017.

Garrett Wilson, Janardhan Rao Doppa, and Diane J. Cook. Multi-source deep domain adaptation with weak supervision for time-series sensor data. In *SIGKDD*, 2020.

Kaichao You, Ximei Wang, Mingsheng Long, and Michael Jordan. Towards accurate model selection in deep unsupervised domain adaptation. In *International Conference on Machine Learning*, pp. 7124–7133. PMLR, 2019.

S. Zhao, Xiangyu Yue, Shanghang Zhang, Bo Li, Han Zhao, B. Wu, R. Krishna, J. Gonzalez, A. Sangiovanni-Vincentelli, S. Seshia, and K. Keutzer. A review of single-source deep unsupervised visual domain adaptation. *IEEE transactions on neural networks and learning systems*, PP, 2020a.

Sicheng Zhao, Xiangyu Yue, Shanghang Zhang, Bo Li, Han Zhao, Bichen Wu, Ravi Krishna, Joseph E Gonzalez, Alberto L Sangiovanni-Vincentelli, Sanjit A Seshia, et al. A review of single-source deep unsupervised visual domain adaptation. *IEEE Transactions on Neural Networks and Learning Systems*, 2020b.

Yongchun Zhu, Fuzhen Zhuang, Jindong Wang, Guolin Ke, Jingwu Chen, Jiang Bian, Hui Xiong, and Qing He. Deep subdomain adaptation network for image classification. *IEEE Transactions on Neural Networks and Learning Systems*, 32(4):1713–1722, 2021. doi: 10.1109/TNNLS.2020.2988928.

# A DETAILED RESULTS OF OUR FRAMEWORK

Here, we provide the detailed results including mean and standard deviation for each cross-domain scenario. It can be clearly seen, that datasets with small sample size suffers from high variance among the different cross-domain scenarios.

Table 4: Detailed results of scenarios of UCIHAR dataset in terms of MF1 score.

| Risk | Algorithm | 17→25 | 12→16 | 9→18 | 6→23 | 7→13 | AVG |
|---|---|---|---|---|---|---|---|
| Target | DDC | 60.0±13.32 | 66.77±8.46 | 61.41±5.80 | 88.55±1.42 | 77.29±2.11 | 75.67 |
| | Deep-Coral | 67.2±13.67 | 64.58±8.72 | 54.38±9.69 | 89.66±2.54 | 90.46±2.96 | 77.71 |
| | HoMM | 83.54±2.99 | 63.45±2.07 | 71.25±4.42 | 94.97±2.49 | 91.41±1.33 | 84.10 |
| | MMDA | 72.91±2.78 | 74.64±2.88 | 62.62±2.63 | 91.14±0.46 | 90.61±2.00 | 81.40 |
| | DSAN | 99.23±1.09 | 65.71±2.92 | 89.69±7.44 | 97.82±1.54 | 94.33±0.00 | 90.96 |
| | DANN | 98.09±1.68 | 62.08±1.69 | 70.7±11.36 | 85.6±15.71 | 93.33±0.00 | 84.97 |
| | CDAN | 98.19±1.57 | 61.20±3.27 | 71.3±14.64 | 96.73±0.00 | 93.33±0.00 | 86.79 |
| | DIRT-T | 98.13±2.64 | 82.05±8.61 | 85.90±6.63 | 93.76±3.10 | 93.35±0.00 | 92.20 |
| | CoDATS | 86.65±4.28 | 61.03±2.33 | 80.51±8.47 | 92.08±4.39 | 92.61±0.51 | 85.47 |
| | AdvSKM | 65.74±2.69 | 60.52±1.99 | 53.25±5.19 | 79.63±8.52 | 88.89±3.12 | 74.67 |
| Few-shot | DDC | 67.95±7.51 | 58.58±1.55 | 48.33±4.06 | 84.34±5.22 | 86.33±2.19 | 74.25 |
| | Deep-Coral | 70.86±5.85 | 59.3±0.77 | 58.5±10.7 | 89.5±1.6 | 85.23±3.01 | 77.23 |
| | HoMM | 78.87±8.37 | 60.34±1.07 | 66.97±3.41 | 93.84±2.04 | 87.82±4.43 | 81.3 |
| | MMDA | 74.36±9.26 | 66.01±5.15 | 54.92±4.27 | 95.88±1.2 | 93.33±0.0 | 79.54 |
| | DSAN | 89.47±8.76 | 65.97±2.59 | 78.02±7.52 | 96.68±2.74 | 92.61±0.51 | 87.13 |
| | DANN | 87.73±5.29 | 60.33±1.9 | 69.69±9.83 | 89.88±6.34 | 93.33±0.0 | 83.10 |
| | CDAN | 98.19±1.57 | 61.2±3.27 | 71.31±14.64 | 96.73±0.0 | 93.33±0.0 | 86.79 |
| | DIRT-T | 92.33±1.49 | 71.63±6.64 | 86.87±0.39 | 86.71±14.17 | 93.33±0.0 | 88.47 |
| | CoDATS | 71.6±15.34 | 65.1±0.68 | 64.51±14.12 | 92.04±4.05 | 81.41±6.04 | 79.10 |
| | AdvSKM | 64.45±2.59 | 61.99±4.07 | 53.13±4.59 | 78.09±9.92 | 88.89±3.12 | 74.47 |
| DEV | DDC | 72.0±3.51 | 59.65±4.11 | 45.42±5.89 | 86.14±1.97 | 81.66±8.07 | 74.14 |
| | Deep-Coral | 67.55±11.65 | 62.13±7.74 | 47.77±2.84 | 72.44±13.45 | 78.7±18.24 | 71.43 |
| | HoMM | 73.38±7.34 | 59.84±1.43 | 60.02±11.83 | 90.48±0.8 | 85.94±2.52 | 78.28 |
| | MMDA | 83.22±3.46 | 62.64±10.42 | 58.43±2.55 | 96.73±0.0 | 94.12±1.11 | 80.12 |
| | DSAN | 75.58±9.18 | 61.71±1.75 | 67.1±4.61 | 93.22±2.49 | 88.82±3.08 | 81.07 |
| | DANN | 77.77±18.26 | 63.26±2.49 | 57.49±7.77 | 95.86±1.84 | 91.71±0.84 | 80.89 |
| | CDAN | 71.51±8.84 | 54.66±2.91 | 40.94±3.18 | 61.31±9.02 | 82.06±11.91 | 64.66 |
| | DIRT-T | 88.44±9.23 | 58.47±2.98 | 65.89±13.25 | 90.56±8.73 | 93.73±0.56 | 82.54 |
| | CoDATS | 51.81±4.67 | 54.81±2.76 | 31.83±8.89 | 81.23±4.07 | 80.98±13.74 | 65.12 |
| | AdvSKM | 65.74±2.69 | 60.09±1.4 | 53.7±4.61 | 79.31±8.95 | 88.89±3.12 | 74.62 |
| Source | DDC | 53.28±5.44 | 64.59±6.34 | 41.99±1.47 | 89.01±2.14 | 85.65±7.92 | 68.83 |
| | Deep-Coral | 62.42±1.97 | 62.19±4.68 | 31.4±7.7 | 88.42±1.01 | 87.84±2.78 | 71.99 |
| | HoMM | 62.95±20.6 | 59.82±0.4 | 53.14±4.71 | 90.04±4.45 | 89.59±4.01 | 75.86 |
| | MMDA | 83.22±3.46 | 62.64±10.42 | 58.43±2.55 | 96.73±0.0 | 94.12±1.11 | 80.12 |
| | DSAN | 84.81±13.2 | 62.91±0.39 | 77.63±0.94 | 81.91±23.31 | 92.97±0.51 | 83.31 |
| | DANN | 70.28±2.86 | 65.45±4.76 | 71.34±6.17 | 90.0±2.71 | 90.51±0.86 | 79.82 |
| | CDAN | 88.73±4.7 | 60.25±4.61 | 81.39±6.15 | 96.73±0.0 | 92.97±0.51 | 86.55 |
| | DIRT-T | 88.44±9.23 | 61.36±2.41 | 78.88±4.12 | 98.64±1.39 | 93.01±0.46 | 86.72 |
| | CoDATS | 71.45±12.93 | 61.98±2.88 | 72.11±4.98 | 96.12±0.86 | 78.92±12.71 | 79.05 |
| | AdvSKM | 69.97±3.68 | 53.73±11.04 | 35.46±8.02 | 85.73±6.11 | 82.29±4.67 | 71.08 |

Table 5: Detailed results of scenarios of WISDM dataset in terms of MF1 score.

| Risk | Algorithm | 35→31 | 7→18 | 20→30 | 6→19 | 18→23 | AVG |
|---|---|---|---|---|---|---|---|
| Target | DDC | 48.85±16.15 | 45.17±6.65 | 70.04±10.28 | 57.51±6.89 | 42.4±8.53 | 52.80 |
| | DeepCoral | 42.36±11.34 | 47.07±7.25 | 67.16±4.86 | 65.06±3.76 | 47.57±8.73 | 53.85 |
| | HoMM | 58.49±7.79 | 53.64±3.48 | 70.94±2.8 | 74.88±6.55 | 56.96±24.07 | 62.98 |
| | MMDA | 54.37±5.23 | 47.75±2.04 | 66.35±2.1 | 76.68±5.71 | 74.7±2.28 | 63.97 |
| | DSAN | 70.35±1.44 | 44.77±4.4 | 69.53±4.91 | 49.85±7.48 | 65.88±7.21 | 60.08 |
| | DANN | 62.53±6.97 | 43.55±2.06 | 53.96±3.03 | 79.05±15.62 | 49.96±5.83 | 57.81 |
| | CDAN | 60.93±8.6 | 58.98±5.36 | 60.43±11.19 | 59.61±0.89 | 49.3±1.05 | 57.85 |
| | DIRT-T | 62.52±10.06 | 68.8±7.94 | 62.31±5.49 | 51.86±6.68 | 67.56±0.51 | 62.61 |
| | CODATS | 74.06±4.77 | 35.8±0.78 | 54.21±4.5 | 45.54±1.33 | 54.0±13.2 | 52.72 |
| | AdvSKM | 55.15±9.56 | 52.36±2.73 | 72.83±3.69 | 58.64±4.33 | 63.78±10.2 | 60.55 |
| Few-shot | DDC | 38.86±14.69 | 43.3±1.8 | 56.56±0.93 | 62.43±7.42 | 49.11±0.23 | 50.05 |
| | Deep Coral | 39.37±15.11 | 45.62±4.25 | 56.86±0.72 | 56.46±5.43 | 48.95±0.19 | 49.45 |
| | HoMM | 35.41±13.8 | 30.52±3.6 | 60.99±1.1 | 54.74±7.85 | 51.15±7.39 | 46.56 |
| | MMDA | 43.47±4.95 | 57.9±1.84 | 55.9±2.97 | 59.8±8.45 | 43.52±8.41 | 52.12 |
| | DSAN | 52.92±14.31 | 51.98±4.93 | 64.35±3.78 | 49.26±7.09 | 48.51±8.15 | 53.41 |
| | DANN | 43.11±9.84 | 43.08±1.21 | 57.63±2.53 | 55.2±4.93 | 48.23±0.4 | 49.45 |
| | CDAN | 54.53±1.31 | 57.03±0.53 | 64.55±6.06 | 39.76±7.63 | 47.85±0.46 | 52.75 |
| | DIRT-T | 68.59±10.7 | 73.57±9.09 | 72.06±8.6 | 50.14±7.43 | 67.03±2.41 | 66.28 |
| | CODATS | 40.68±24.05 | 37.82±2.61 | 61.01±1.2 | 56.3±8.87 | 47.38±1.23 | 48.64 |
| | AdvSKM | 57.43±12.5 | 73.58±1.33 | 71.2±3.2 | 78.28±3.05 | 67.78±0.79 | 49.02 |
| DEV | DDC | 51.84±5.68 | 43.56±0.66 | 65.83±2.04 | 62.58±2.72 | 51.36±10.81 | 55.03 |
| | Deep Coral | 56.48±8.18 | 44.32±1.79 | 66.33±2.17 | 63.11±3.17 | 56.91±3.24 | 57.43 |
| | HoMM | 66.29±0.84 | 48.67±6.31 | 65.3±2.45 | 63.78±4.35 | 62.11±7.57 | 61.23 |
| | MMDA | 60.34±7.52 | 41.58±8.79 | 64.39±4.28 | 55.74±3.88 | 64.47±10.75 | 57.30 |
| | DSAN | 57.25±6.07 | 52.77±2.23 | 63.4±0.7 | 53.35±5.37 | 55.76±1.46 | 56.51 |
| | DANN | 52.21±1.09 | 41.16±6.62 | 71.96±10.1 | 59.09±3.57 | 48.0±0.9 | 54.48 |
| | CDAN | 49.02±4.2 | 57.65±0.18 | 65.5±0.61 | 44.03±0.81 | 50.16±0.44 | 53.27 |
| | DIRT-T | 46.75±3.54 | 57.89±0.15 | 65.49±0.62 | 45.16±0.0 | 50.9±0.4 | 53.24 |
| | CODATS | 40.96±19.0 | 42.0±3.75 | 69.65±7.6 | 70.59±12.51 | 48.15±15.11 | 54.27 |
| | AdvSKM | 61.91±6.95 | 49.84±5.31 | 69.35±1.38 | 54.89±4.14 | 51.3±10.33 | 57.46 |
| Source | DDC | 51.47±5.69 | 43.65±0.78 | 65.83±2.04 | 62.58±2.72 | 51.36±10.81 | 54.98 |
| | Deep Coral | 53.46±7.12 | 43.65±0.78 | 66.08±2.05 | 63.16±3.14 | 51.36±10.81 | 55.54 |
| | HoMM | 57.94±7.0 | 43.23±0.53 | 65.47±1.13 | 63.91±4.12 | 56.91±3.24 | 57.49 |
| | MMDA | 61.44±6.08 | 49.79±6.76 | 67.82±1.37 | 60.83±0.27 | 47.78±5.98 | 57.53 |
| | DSAN | 57.25±6.07 | 52.77±2.23 | 63.4±0.7 | 53.35±5.37 | 55.76±1.46 | 56.51 |
| | DANN | 46.56±11.92 | 44.04±2.61 | 68.13±1.27 | 54.41±4.61 | 52.92±2.86 | 53.21 |
| | CDAN | 44.25±6.84 | 57.44±7.58 | 63.67±0.63 | 47.81±5.88 | 49.27±0.12 | 52.49 |
| | DIRT-T | 72.59±4.03 | 57.74±0.06 | 53.47±2.17 | 60.91±0.38 | 57.46±8.41 | 60.43 |
| | CODATS | 50.93±5.46 | 51.21±5.66 | 67.28±3.2 | 65.24±3.68 | 49.1±10.92 | 56.75 |
| | AdvSKM | 42.3±16.63 | 53.66±5.72 | 62.59±2.7 | 60.37±0.81 | 50.84±2.66 | 53.95 |

Table 6: Detailed results of scenarios of SSC dataset in terms of MF1 score.

| Risk | Algorithm | 16→1 | 9→14 | 12→5 | 7→18 | 0→11 | AVG |
|---|---|---|---|---|---|---|---|
| Target | DDC | 55.47±1.72 | 63.57±1.43 | 55.43±2.75 | 67.46±1.45 | 54.17±1.79 | 61.44 |
| | Deep-Coral | 55.50±1.74 | 63.50±1.36 | 55.35±2.64 | 67.49±1.50 | 53.76±1.89 | 61.39 |
| | DANN | 58.68±3.29 | 64.29±1.08 | 64.65±1.83 | 69.54±3.00 | 44.13±5.84 | 59.95 |
| | HoMM | 55.51±1.79 | 63.49±1.14 | 55.46±2.71 | 67.50±1.50 | 53.37±2.47 | 61.22 |
| | CDAN | 59.65±4.96 | 64.18±6.37 | 64.43±1.17 | 67.61±3.55 | 39.38±3.28 | 59.26 |
| | MMDA | 62.92±0.96 | 71.04±2.39 | 65.84±1.08 | 70.95±0.82 | 43.23±4.31 | 61.41 |
| | DSAN | 59.87±2.84 | 70.71±2.79 | 65.55±0.79 | 68.44±1.39 | 38.28±3.57 | 61.39 |
| | DIRT-T | 61.31±4.23 | 66.39±4.86 | 66.95±1.72 | 70.51±0.89 | 33.05±2.49 | 59.95 |
| | CoDATS | 63.84±3.36 | 63.51±6.92 | 52.54±5.94 | 66.06±2.48 | 46.28±5.99 | 56.41 |
| | AdvSKM | 57.68±0.79 | 64.31±2.93 | 55.29±2.58 | 67.22±3.9 | 55.16±4.39 | 60.32 |
| Few-shot | DDC | 55.48±1.76 | 63.54±1.33 | 55.32±2.94 | 67.5±1.5 | 54.28±1.68 | 61.48 |
| | Deep-Coral | 55.5±1.84 | 63.55±1.33 | 55.42±2.66 | 67.53±1.54 | 52.1±2.85 | 61.42 |
| | DANN | 58.68±3.3 | 64.3±1.08 | 64.65±1.83 | 69.54±3.0 | 44.13±5.84 | 60.61 |
| | HoMM | 55.51±1.79 | 63.5±1.14 | 55.46±2.71 | 67.5±1.5 | 53.37±2.47 | 61.31 |
| | CDAN | 59.87±2.67 | 63.55±3.16 | 62.13±1.8 | 64.12±0.48 | 31.19±8.26 | 60.78 |
| | MMDA | 65.63±0.67 | 65.92±4.44 | 57.99±6.43 | 71.5±0.97 | 28.9±3.78 | 62.23 |
| | DSAN | 56.39±0.67 | 63.85±0.63 | 62.47±2.6 | 68.92±1.67 | 43.25±2.76 | 62.28 |
| | DIRT-T | 56.33±5.86 | 65.15±1.99 | 64.88±5.58 | 69.83±1.57 | 34.99±0.54 | 60.95 |
| | CoDATS | 59.84±0.64 | 53.02±4.53 | 57.58±1.75 | 55.12±3.55 | 47.64±2.4 | 58.45 |
| | AdvSKM | 57.83±1.42 | 64.76±3.0 | 55.73±1.42 | 67.58±3.64 | 55.2±4.19 | 60.36 |
| DEV | DDC | 55.53±1.87 | 63.57±1.26 | 55.35±2.73 | 67.46±1.55 | 54.14±1.7 | 61.39 |
| | Deep-Coral | 55.5±1.84 | 63.55±1.33 | 55.42±2.66 | 67.5±1.5 | 52.1±2.85 | 61.36 |
| | DANN | 58.78±4.76 | 64.61±0.93 | 65.47±0.95 | 68.88±2.81 | 31.13±1.74 | 57.96 |
| | HoMM | 55.57±2.0 | 63.66±1.48 | 55.87±2.93 | 67.49±1.51 | 50.93±4.31 | 60.95 |
| | CDAN | 60.95±1.13 | 60.54±10.01 | 65.0±1.34 | 67.02±1.13 | 30.79±10.69 | 60.42 |
| | MMDA | 63.44±1.49 | 67.14±4.78 | 64.93±1.21 | 71.89±1.44 | 39.88±4.96 | 61.49 |
| | DSAN | 58.76±2.02 | 69.45±4.04 | 64.92±1.65 | 68.69±0.99 | 37.43±2.9 | 61.70 |
| | DIRT-T | 54.42±12.46 | 71.33±3.72 | 64.99±4.98 | 69.94±0.43 | 35.62±3.79 | 60.58 |
| | CoDATS | 60.03±1.18 | 52.22±10.55 | 56.96±2.4 | 68.64±2.93 | 41.1±5.14 | 55.79 |
| | AdvSKM | 57.8±0.69 | 64.27±2.93 | 55.12±2.52 | 67.31±3.83 | 55.11±4.56 | 60.35 |
| Source | DDC | 55.48±1.76 | 63.57±1.29 | 55.16±2.76 | 67.5±1.5 | 54.24±1.79 | 61.11 |
| | Deep-Coral | 55.5±1.74 | 63.5±1.36 | 55.35±2.64 | 67.5±1.5 | 53.76±1.89 | 61.42 |
| | DANN | 58.68±3.3 | 64.3±1.08 | 64.65±1.83 | 69.54±3.0 | 44.13±5.84 | 60.61 |
| | HoMM | 55.51±1.79 | 63.5±1.14 | 55.46±2.71 | 67.5±1.5 | 53.37±2.47 | 61.31 |
| | CDAN | 62.06±0.91 | 63.32±5.02 | 48.8±1.02 | 63.46±1.18 | 36.86±8.23 | 57.86 |
| | MMDA | 59.6±0.51 | 68.25±4.17 | 65.63±0.85 | 71.06±0.99 | 45.89±1.97 | 62.13 |
| | DSAN | 63.05±3.14 | 63.84±10.11 | 57.55±11.16 | 68.84±2.25 | 37.46±4.76 | 61.46 |
| | DIRT-T | 59.11±3.24 | 65.08±1.42 | 65.5±4.92 | 67.27±1.58 | 35.29±2.92 | 59.38 |
| | CoDATS | 56.52±1.76 | 68.2±5.72 | 59.72±6.66 | 63.31±3.9 | 36.05±8.95 | 56.76 |
| | AdvSKM | 57.78±0.72 | 64.29±2.97 | 55.15±2.52 | 67.33±3.82 | 55.16±4.4 | 60.34 |

## B CLASS DISTRIBUTION OF DIFFERENT SUBJECTS

In this section, we visualize the class distribution of each selected subjects for all the datasets.

(a) HAR dataset

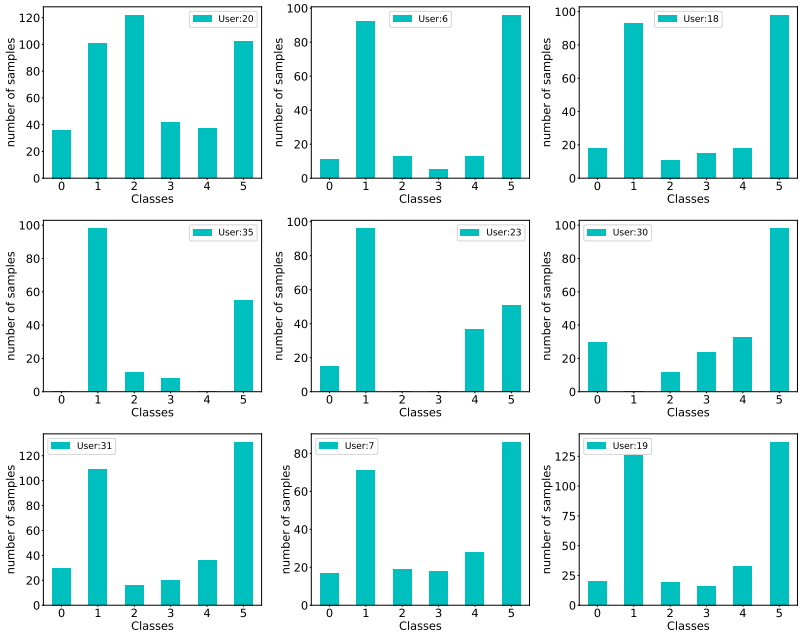


(b) WISDM dataset

Figure 4: Class distribution of selected subjects among different datasets

## C HYPER-PARAMETER IMPORTANCE

The importance of each hyper-parameter can be valuable when you have low budget for hyper-parameter tuning. As such you can tune the most important hyper-parameter while fixing others to specific value. In this work, We also study how different hyper-parameters can affect the model performance. We test the learning rate against other model specific performance for 5 different domain adaptation algorithms. To do so, we leverage random forest model and feed the corresponding hyper-parameters as input and the target metric as output (Probst et al., 2019). In our case, we averaged all the model selection risks and use them as a metric to calculate the importance of each parameter.

Figure 5, we study the effect of learning rate, as well as the weights of domain alignment loss (differs according to each method) and the source classification loss. We calculate the importance of these parameters while running the sweeps of three different methods i.e., DDC, Deep-CORAL and AdvSKM. We find that the learning rate is the most significant parameter especially with SSC dataset, as it contributes with more than 80% of the performance. We conclude that more effort should be put in finding the best learning rate that suites each dataset. In addition, we find that the source classification loss comes next in the importance, and hence, more weight should be assigned to it.

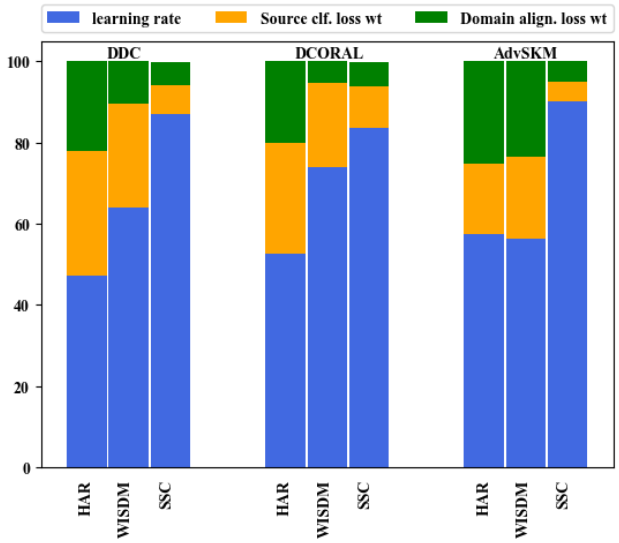


Figure 5: Parameters importance for some selected UDA methods through the three datasets.

## D DETAILED PARAMETER RANGES FOR THE HYPER-PARAMETER SEARCH

Here, we provide the detailed ranges for each parameter among all selected domain adaptation methods.

Table 7: Details of hyper-parameter tuning setup.

| **Method** | **Hyperparameter** | **Range** |
|---|---|---|
| | Learning Rate | $10^{-2}$ to $10^{1}$ |
| DDC | MMD loss | $10^{-2}$ to $10^{1}$ |
| | Classification loss | $10^{-1}$ to $10^{1}$ |
| Deep CORAL | Coral loss | $10^{-2}$ to $10^{1}$ |
| | Classification loss | $10^{-1}$ to $10^{1}$ |
| HoMM | High-order-MMD loss | $10^{-2}$ to $10^{1}$ |
| | Classification loss | $10^{-1}$ to $10^{1}$ |
| MMDA | MMD loss | $10^{-2}$ to $10^{1}$ |
| | Coral Loss | $10^{-2}$ to $10^{1}$ |
| | Conditional loss | $10^{-2}$ to $10^{1}$ |
| | Classification loss | $10^{-1}$ to $10^{1}$ |
| DSAN | Local MMD loss | $10^{-2}$ to $10^{1}$ |
| | Classification loss | $10^{-2}$ to $10^{1}$ |
| DANN | MMD loss | $10^{-2}$ to $10^{1}$ |
| | Classification loss | $10^{-1}$ to $10^{1}$ |
| CDAN | Adversarial loss | $10^{-2}$ to $10^{1}$ |
| | Conditional loss | $10^{-2}$ to $10^{1}$ |
| | classification loss | $10^{-1}$ to $10^{1}$ |
| DIRT-T | Adversarial loss | $10^{-2}$ to $10^{1}$ |
| | Conditional loss | $10^{-2}$ to $10^{1}$ |
| | virtual adversarial | $10^{-2}$ to $10^{1}$ |
| | Discriminator steps | $10^{-2}$ to $10^{1}$ |
| | classification loss | $10^{-1}$ to $10^{1}$ |
| CODATS | Adversarial loss | $10^{-2}$ to $10^{1}$ |
| | classification loss $\alpha$ | $10^{-1}$ to $10^{1}$ |
| AdvSKM | Adversarial MMD loss | $10^{-2}$ to $10^{1}$ |
| | Classification loss | $10^{-1}$ to $10^{1}$ |

## E BACKBONE NETWORK ARCHITECTURE

Here, we present the detailed architecture of ADATIME backbone network.

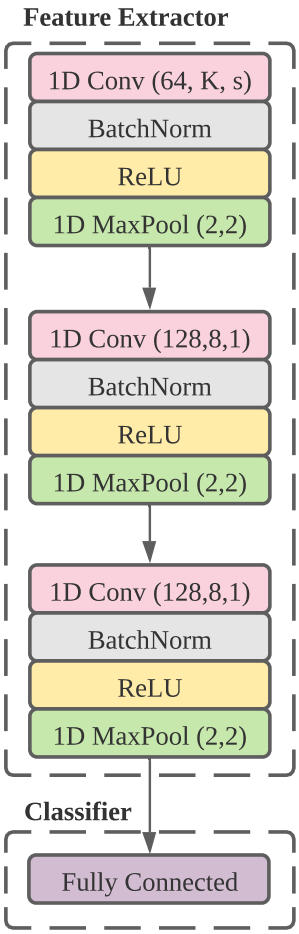


Figure 6: Backbone network of our ADATIME, where $K$ is the kernel size and $s$ is the stride.